

21 Rhine-Meuse Estuary forms an ideal study site, as over 100 scour holes have been identified in
22 this area and over 40 years of bed level data and thousands of core description are available. It is
23 shown that the subsurface lithology plays a crucial role in the emergence of scour holes, their shape
24 and evolution. Although most scour holes follow the characteristic exponential development of
25 fast initial growth and slower final growth, temporally strong variations are observed, with sudden
26 growth rates of several meters per year in depth and tens of meters in extent. In addition, we could
27 relate the characteristic build-up of the subsurface lithology to typical scour hole development like
28 large elongated expanding scour holes or confined scour holes with steep slopes. As river deltas
29 commonly have a heterogeneous substratum and often face channel bed erosion, the observations
30 likely apply to many delta rivers. These findings call for good knowledge of the subsurface
31 lithology as without, scour hole development is hard to predict and can lead to sudden failures of
32 nearby infrastructure and flood defence works.

33 **1 Introduction**

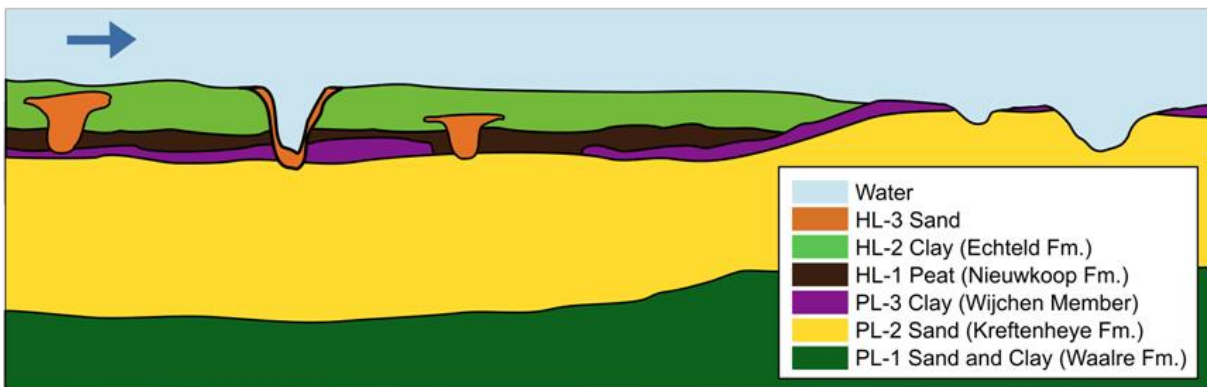
34 Scour holes are common features to occur in rivers and estuaries. With their steep slopes
35 and large depths, these scour holes can form a risk for the stability of nearby structures and
36 infrastructure like embankments, bridge piers, tunnels and pipelines (e.g. Beltaos et al., 2011;
37 Gharabaghi et al., 2007; Liang et al., 2020; Pandey et al., 2018; Wang et al., 2017). The formation
38 and development of local scour, bend scour and confluence scour are widely studied (e.g. Andrlé,
39 1994; Beltaos et al., 2011; Best, 1986; Best & Rhoads, 2008; Blanckaert, 2010; Engelund, 1974;
40 Ferrarin et al., 2018; Gharabaghi et al., 2007; Ginsberg & Perillo, 1999; Kjerfve et al., 1979; Liang
41 et al., 2020; Mosley, 1976; Odgaard, 1981; Ottevanger et al., 2012; Pandey et al., 2018; Pierini et
42 al., 2005; Vermeulen et al., 2015; C. Wang et al., 2017; Zimmermann & Kennedy, 1978, 1978).
43 These studies however generally focus on scour hole development in a homogeneous sandy

44 subsurface. The influence of heterogeneities in the subsurface lithology on scour hole formation is
45 hardly studied, while this may greatly impact the scour hole evolution or even induce scour hole
46 formation (Figure 1), provided there is enough hydraulic forcing. In case of large-scale bed
47 degradation in channel beds composed of fluvial sand and with no constructions or local river
48 narrowing, erosion is evenly distributed. However, when the substratum is composed of layers
49 with strongly varying erodibility, local depressions form at locations with higher erodibility
50 (Cserkés-Nagy et al. 2010; Huismans et al. 2016; Sloff et al. 2013).

51 Many of world's large rivers in deltas face channel bed degradation. Examples are the
52 Yangtze, the Rhine-Meuse Estuary, the Mississippi and the Mekong rivers (Luan et al. 2016;
53 Brunier et al. 2014; Galler et al. 2003; Hoitink et al. 2017; Sloff et al. 2013; Wang and Xu 2018).
54 Causes are mainly anthropogenic and range from extracting sediment by dredging and sand
55 mining, a reduction in sediment supply due to the presence of upstream dams and levees and
56 interventions that enhance flow velocities. As river deltas commonly have a heterogeneous
57 substratum of alternating peat, clay and sand deposits (e.g. Aslan & Autin, 1999; Aslan et al.,
58 2005; Berendsen & Stouthamer, 2001, 2002; Cohen et al., 2012; Gouw & Autin, 2008; Hanebuth
59 et al., 2012; Kuehl et al., 2005.; Stefani & Vincenzi, 2005) and are among the regions with the
60 highest population density (Best 2019; Syvitski et al. 2009), understanding how the lithology
61 controls the scour hole development is highly relevant.

62 One of the first papers to discuss the influence of a heterogenous subsurface lithology on
63 the channel bed morphology is by Nittrouer et al. (2011). Based on multibeam surveys, high
64 intensity radar pulse seismic data and grab samples, they map five sediment facies for the
65 lowermost Mississippi river, of which three consisting of modern alluvial deposits and two of relict
66 substratum. They show that the sediment facies associated with relict substratum are mainly

67 exposed in the regions with the most erosion, namely the deeper parts of the channel bed and at
68 the sidewalls of the outer bends. Erosion of the sidewall substratum is furthermore inhomogeneous,
69 due to the spatially heterogeneous fluvio-deltaic sedimentary deposits that have variable resistance
70 to erosion. Cserkés-Nagy et al. (2010) show a strong lithological control on the erosion and lateral
71 migration of the Tisza river (Hungary) in response to engineering measures. Erosion is either found
72 to be promoted, in case sandy deposits are incised, or suppressed when resistant silty-clayey
73 substratum prohibits further erosion. For the Ems estuary (Pierik et al., 2019) demonstrate how the
74 composition of the subsurface lithology controlled the evolution of eb-tide channels over a 200
75 years timespan. The clear link to the emergence of scour holes is made by Sloff et al. (2013), who
76 observed deep scour holes in the Rhine-Meuse estuary and demonstrated the principle of scour
77 hole formation in heterogeneous subsurface both conceptually as with a numerical model. In a
78 follow up paper by Huismans et al. (2016), the link between scour hole occurrence and the
79 composition of the subsurface lithology was directly made, by combining multibeam surveys and
80 detailed geological maps constructed based on lithological data from corings.



81
82 *Figure 1. Conceptual longitudinal subsurface lithological section of a river bed. Arrow indicates flow direction. Scour*
83 *holes form in layers or patches composed of sandy material with lower erodibility compared to the surrounding*
84 *resistant clay or peat layers.*

85

86 This paper builds on the work of Huisman et al. (2016), by analysing in detail how the
87 subsurface lithology influences the bed elevation in net incising river branches, particularly
88 focusing on scour hole initiation, growth rate, direction and shape, as this is essential information
89 in judging whether scour holes form a risk for the stability of river banks, dikes or other nearby
90 infrastructure. The Rhine-Meuse Estuary in the Netherlands forms an ideal study area, as more
91 than a hundred scour holes are identified in this area, of which many are expected to be influenced
92 or triggered by heterogeneities in the subsurface lithology (Huisman et al., 2016). In addition,
93 over 40 years of yearly single- and multibeam data and lithological data from many corings are
94 available. This allows analysing decades of bed level evolution and linking it to the subsurface
95 composition. Upon identifying how the location, growth direction and rates are influenced by the
96 heterogeneity of the subsurface lithology, first a reconstruction of the subsurface lithology is made
97 based on thousands of core descriptions along the main river branches of the Rhine-Meuse Estuary.
98 Subsequently the recent 5-year scour hole growth is mapped for the set of over 100 scour holes.
99 For a subset of 18 scour holes, the evolution since 1976 is analysed and linked to the subsurface
100 lithology. In a final step, scour hole characteristics in three sub-reaches with distinct lithological
101 composition are analysed, highlighting the differences in lithological control on the size, growth
102 rate and direction of scour holes.

103 **2 Study Area**

104 The Rhine-Meuse Estuary is located in the western part of the Netherlands, where the rivers
105 Rhine and Meuse debouch into the North Sea (Figure 2). During the Late Pleistocene Younger
106 Dryas stadial (12.900-11.700 cal yr. BP), the area consisted of a wide braided river valley. During
107 the early Holocene (11.700 - 8.200 cal yr. BP), the braided river system gradually transformed into

108 a meandering system, due to climatic warming and restoration of vegetation (Berendsen &
109 Stouthamer, 2000; Berendsen et al., 1995; Cohen, 2003; Gouw & Erkens, 2007; Hijma, 2009;
110 Janssens et al., 2012; Pons, 1957). The sandy sediments deposited by the braided rivers,
111 predominantly consist of gravel and coarse sand (Kreftenheye Fm., PL-2, Figure 1). At the top,
112 finer grained sand is found, with grain sizes varying from 150 μm to 300 μm (Vos & Cohen, 2014).
113 During flood events fine sediments were deposited on the floodplains, forming a strong resistant
114 silty clay loam layer (Wijchen Member, PL-3) (Busschers et al. 2007; Hijma et al. 2009; Törnqvist
115 et al. 1994). In most of the study area, this silty clay loam layer (Wijchen Mb.) covers the
116 Pleistocene sandy deposits. Due to rapid early Holocene sea level rise, the area changed from a
117 wide river valley into an estuary (T. de Haas et al., 2018; Hijma, 2009). During this stage peat
118 lands formed in response to the higher ground water tables (Nieuwkoop Fm., HL-1), which
119 regionally got covered by clay from tidal deposits in the west (Naaldwijk Fm.) and floodplain
120 deposits in the east (Echteld Fm., HL-2) (Hijma et al., 2009). The rapid growth in accommodation
121 space triggered a peak in avulsion frequency around 8000 – 7200 cal yr. BP (Stouthamer &
122 Berendsen, 2000; Stouthamer et al., 2011a). A second peak in avulsion frequency occurred around
123 3300-1800 cal yr. BP and was triggered from upstream, where due to deforestation the sediment
124 supply to the river doubled (Erkens, 2009; Stouthamer & Berendsen, 2000). During this time, a
125 major avulsion caused the Rhine to shift its mouth from the area near Leiden to the south near
126 Rotterdam, close to its current outlet position (Figure 3a) (Berendsen & Stouthamer, 2000; De
127 Haas et al., 2019; Pierik et al., 2018). A detailed geological mapping of the past river course
128 development is available for the entire Rhine-Meuse Delta (Cohen et al., 2012), showing where
129 the river and tidal channel deposits are preserved in the subsurface lithology (HL-3).



130

131 *Figure 1 Overview of the river channels forming the Rhine-Meuse Estuary (the Netherlands). In colour the bed level*
 132 *is represented (year 2013, 2014). Map is created in QGIS with the Esri-TOPO base map.*

133 Since the High Middle Ages (~1000 AD), human impacts on the delta increased.
 134 Floodplains were cultivated, parts of the peat land excavated, and rivers were constraint by dikes.
 135 This was followed by major changes to the river planform, when in the second half of the
 136 19th century, two new channels were constructed, the Nieuwe Merwede and Nieuwe Waterweg
 137 (Figure 2). Since that time, continuous deepening of channels and closure or reconstruction of river
 138 branches impacted the Rhine-Meuse Estuary. The most recent large intervention is the closure of
 139 one of its tidal outlets in 1970, the Haringvliet (Figure 2). The latter caused a major change in the
 140 hydrodynamics (Vellinga et al., 2014), leading to enhanced flow velocities in the connecting
 141 channels which triggered severe erosion (Hoitink et al. 2017; Sloff et al., 2013) of up to several
 142 meters in about 40 years' time (this paper). In the southern part of the estuary, flow velocities
 143 strongly decreased, which resulted in sedimentation of mostly fine silt.

144 Nowadays the Rhine-Meuse Estuary carries an average annual discharge of 2110 m³/s, of
145 which 1590 m³/s exits through its main outlet, the Maasmond, and 510 m³/s through the
146 Haringvliet sluices (average values in timeframe 2006-2015). During high river discharges, the net
147 river discharge can reach up to about 10.000 m³/s, while during dry periods it may drop below
148 600 m³/s. During low discharge events the Haringvliet sluices entirely close and all water leaves
149 the system via the Maasmond to restrain salt intrusion in the Maasmond and ensure the fresh water
150 supply in the estuary.

151 The Rhine-Meuse Estuary receives sediment from both the North Sea and its upstream
152 river branches Waal, Lek and Maas. The marine input of sand, silt and clay is estimated at
153 5.8 Mt/year, while only 1.3 Mt/year of sediment is exported to sea (Frings et al., 2019). Though
154 these numbers have a large uncertainty, the marine input is certainly large compared to the
155 combined input of all upstream river branches, which is 2.6 Mt/year (Frings et al., 2019). These
156 numbers show the system has a natural trend to import sediment. However, as dredging exceeds
157 the sediment import, the Rhine-Meuse Estuary loses net sediment.

158 The genesis of the area with avulsions, infilling and abandoning channels and development
159 of marshes, has resulted in a heterogeneous substratum composed of layers and patches of sand,
160 clay and peat. The grain size distribution and sediment characteristics of the top layer of the
161 channel bed, vary strongly within the system. In the easterly branches (Beneden Merwede, Nieuwe
162 Merwede, Lek, Bergsche Maas), the top layer is mostly sandy, with median grain sizes ranging
163 from 0.25 to 4 mm (Frings et al., 2019; Fugro, 2002). Locally the top layer consists of erosion
164 resistant peat or clay. In the southern part (Haringvliet, Hollandsch Diep, Amer), silt and clay
165 contents dominate the bed, of which most has settled since the closure of the Haringvliet by a gated
166 barrier in 1976. In the connecting branches (Oude Maas, Noord, Dordtsche Kil, Spui), large areas

167 of erosion resistant clay and peat form the top layer, but also areas with sand or silt are found
168 (Frings et al., 2019; Fugro, 2002).

169 **3 Data and methods**

170 To investigate the influence of the subsurface lithology on scour hole initiation, growth
171 rate and direction, an extensive set of geological data and bed level data is analysed. The method
172 in essence consists of analysing and interpreting the geological records to reconstruct the
173 subsurface lithology and analysing single and multi-beam surveys to evaluate the bed level
174 evolution and scour hole growth in relation to the lithology. The subsurface lithology
175 reconstruction resulted in longitudinal lithological sections along the centrelines of most of the
176 river branches. The data-analysis of the bed level surveys is carried out in three phases. First a
177 general overview is created, by mapping the recent five-year growth characteristics for all scour
178 holes in the estuary. Secondly, for two branches the evolution of the overall bed level since 1976
179 has been analysed, as well as the growth rates of their scour holes. The observed trends are linked
180 to the subsurface lithology. In the last step, three distinct scour holes are analysed in full detail.
181 These three scour holes distinguish in growth rate, growth direction and size, which can be related
182 to differences in surrounding geological layers.

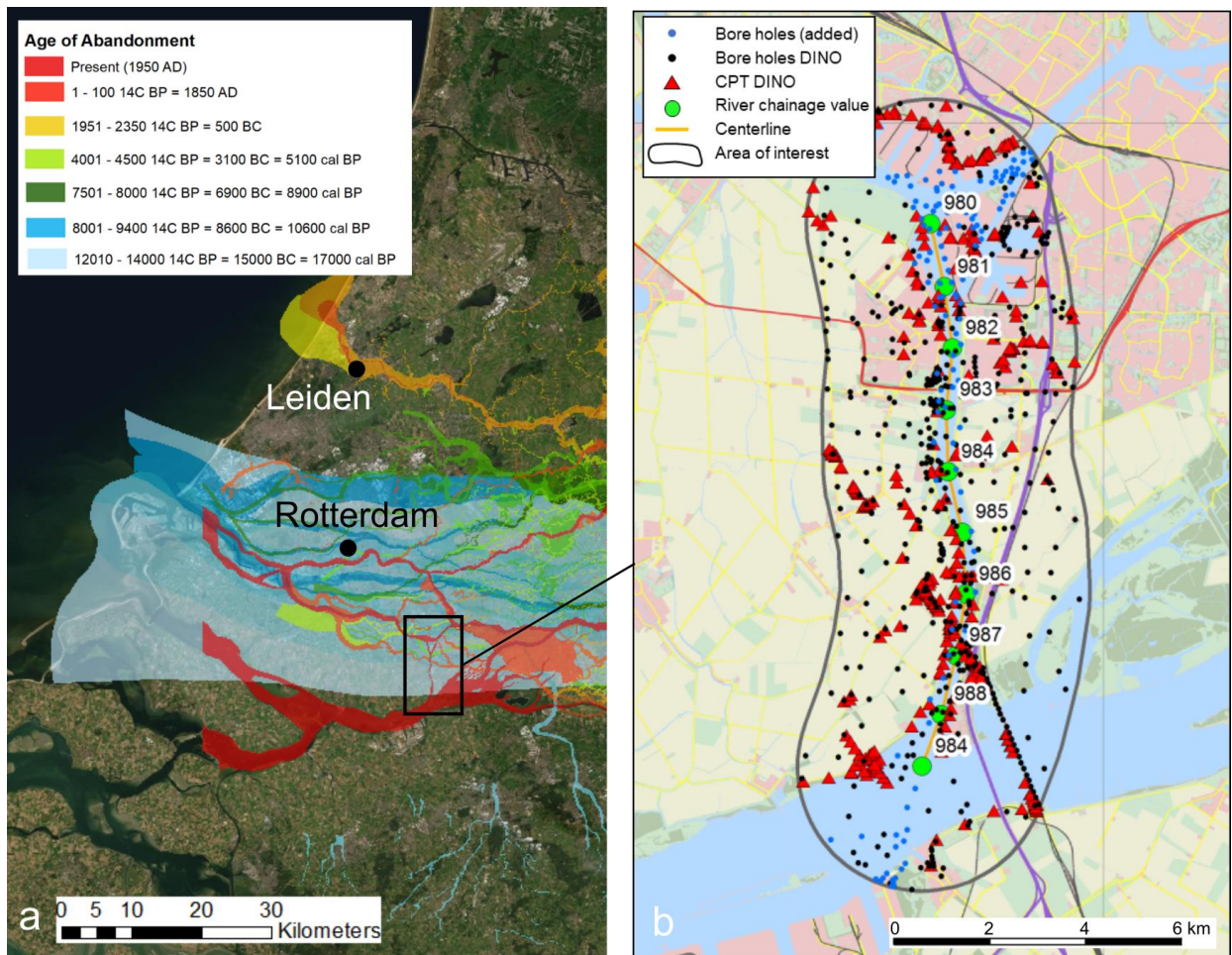
183

184 **3.1 Subsurface lithology**

185 The main source of geological data is the digital DINO-database with lithological core
186 descriptions (TNO, 2010, 2014). For the area of interest, core descriptions from within a range of
187 2 km of the river channel are selected (Figure 3). Most descriptions are from cores taken next to
188 the river channel. For the river branches Dordtsche Kil, Nieuwe Maas, Boven Merwede and the

189 Nieuwe Waterweg about 684 lithological core descriptions and grab samples taken within the river
190 are available, which originate from the Deltadienst and the Dutch Directorate-General for Public
191 Works and Water Management (Rijkswaterstaat) and its predecessors, and which are added to the
192 DINO-database. In addition to the core descriptions, the Digital Basemap for Delta evolution and
193 Paleogeography of the Rhine-Meuse Delta (Cohen et al., 2012) is used for the location and age of
194 the channel belts. The mapping of the channel belts is based on cores from Utrecht University and
195 the DINO-database, lidar imagery (www.ahn.nl), and sedimentological and geomorphological
196 principles. The dating is based on a combination of archaeological findings, C14 dating, historical
197 sources and maps, and geological cross-cutting principles. The third source used is the 3D
198 geological GeoTOP model (Stafleu et al., 2011), which for each voxel of 100 x 100 x 0.5 m,
199 contains information on the lithostratigraphy and lithological classes up to a depth of 50 m below
200 NAP (Dutch Ordnance Level).

201 Based on the core descriptions, cone penetration tests, channel belt mapping, GeoTOP
202 results and previous paleogeographic reconstruction of the delta (Hijma & Cohen, 2011; Hijma et
203 al., 2009), lithological long and cross sections are constructed for the Nieuwe Waterweg, Nieuwe
204 Maas, Oude Maas, Noord, Dordtsche Kil, Spui, Merwedede and Lek (Huisman et al., 2013;
205 Stouthamer & De Haas, 2011; Stouthamer et al., 2011b-d; Wiersma, 2015).



206

207 *Figure 3 Overview of the main data sources used for the reconstruction of the subsurface lithology, a) overview of the*
 208 *age of abandonment of Holocene channel belts (Cohen et al., 2012), map created with ArcGIS and with World Imagery*
 209 *used as background (Esri, Maxar, Earthstar Geographics, CNES/Airbus DS, USDA FSA, USGS, AeroGRID, IGN, IGP,*
 210 *and the GIS User Community), b) overview of the available core descriptions and cone penetration tests for the*
 211 *Dordtsche Kil river (Wiersma, 2015).*

212 3.2 Bed level

213 For the analysis of the bed level evolution, single beam data is available for the period
 214 1976 – 2005 and multibeam surveys are available from 2006 onwards, all provided by the Dutch
 215 Directorate-General for Public Works and Water Management. For the period 1976 – 1993, the
 216 single-beam data consists of yearly cross sections at every 100 m to 125 m, with 10 m spacing

217 between each measurement point within each cross section. For the period 1994 – 1999, cross
218 sections are measured at every 25 m to 100 m with generally 1 m spacing between each
219 measurement point within the cross section. During this period, some areas were surveyed more
220 intensively with both cross and longitudinal sections. From the year 2000 the resolution increases
221 and the provided single beam measurements are interpolated onto a 5 x 5 m grid. The multi-beam
222 data from 2006 onwards consist of yearly surveys and are available on a 1 x 1 m resolution grid.
223 For areas that are surveyed more frequently, the last measured value is taken.

224 In the first step of the analysis, the growth characteristics over the period 2009 - 2014 are
225 determined for all scour holes identified in the study of Huisman et al. (2016). This database
226 consists of 81 scour holes, or groups of scour holes if they are located close to each other. In the
227 analysis all individual scour holes are regarded, such that in total 107 scour holes are analysed.
228 Due to insufficient data for the river branches Haringvliet and Brabantsche Biesbosch, the scour
229 holes in those branches were left out from the analysis. Based on the multi-beam measurements
230 from 2009 and 2014 the change in extent and depth over 5 years' time is determined. The change
231 in depth is defined as the difference between the level of the deepest point in 2009 and 2014. Note
232 that the location of the deepest point may change over time. The change in extent is based on the
233 evolution of the depth contour that marks the area of the scour hole.

234 The analysis subsequently zooms in onto two branches, the Dordtsche Kil and Oude Maas.
235 For these branches the bed level evolution from 1976 to present is analysed, by plotting the
236 maximum depth along the river. For each river chainage value interval, the deepest point over the
237 width of the river is determined. For the single beam, the maximum depth per measured cross
238 section is taken, which results in resolution between 25 m to 125 m, depending on the spacing of
239 the original single beam tracks. For the interpolated single beam data and multibeam data the

240 deepest point per river chainage value is taken with an interval of 100 m for 2000 and 2004 and
241 10 m for all other years.

242 To evaluate the depth development of the scour holes of the Dordtsche Kil and Oude Maas
243 between 1976 and 2015, the deepest point within the scour hole is plotted against time. This
244 enables to determine whether a scour hole grows steadily in depth or whether it faces a sudden
245 acceleration or deceleration in growth, and whether it is reaching its equilibrium depth. Because
246 the size of the scour holes may be comparable to the distance between the various single beam
247 cross sections, only points within a range of 50 m from the current deepest point of the scour hole
248 are considered.

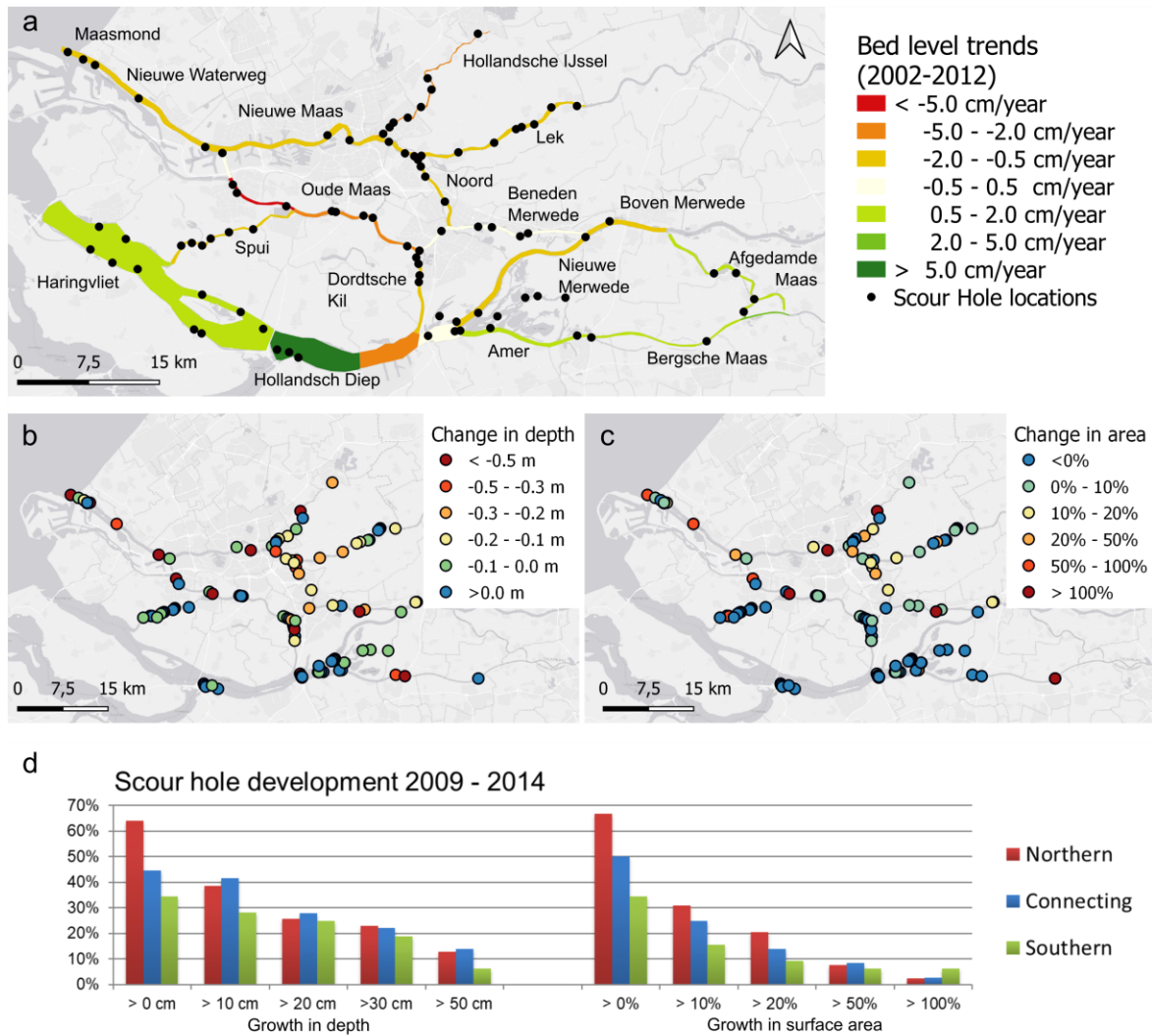
249 In the last step of the analysis three reaches are analysed in full detail. For this, multi-beam
250 data is visualized in GIS. To clearly distinguish the structures in the river bed “hill shade” is used.

251 **4 Results**

252 4.1 Recent growth characteristics of all scour holes

253 An overview of the scour holes in the Rhine-Meuse Estuary is given in Figure 4, together
254 with the bed level trends, as taken from the most recent sediment budget of the Rhine-Meuse
255 Estuary (Becker, 2015) for the period 2002-2012. Scour holes are found in all river channels
256 throughout the entire delta, even in branches that are aggrading. Scour holes in these branches are
257 presumably related to either the presence of structures like bridge piers, which cause local scour,
258 or are relics of old tidal channels that have not been infilled yet.

259 The overview of the scour hole development between 2009-2014 (Figure 4), shows that
260 most of the scour holes still grow in depth or extent. Only about 10% of the scour holes shows a
261 depth increase of more than 50 cm or an increase in extent of more than 50% over 5 years' time.



262

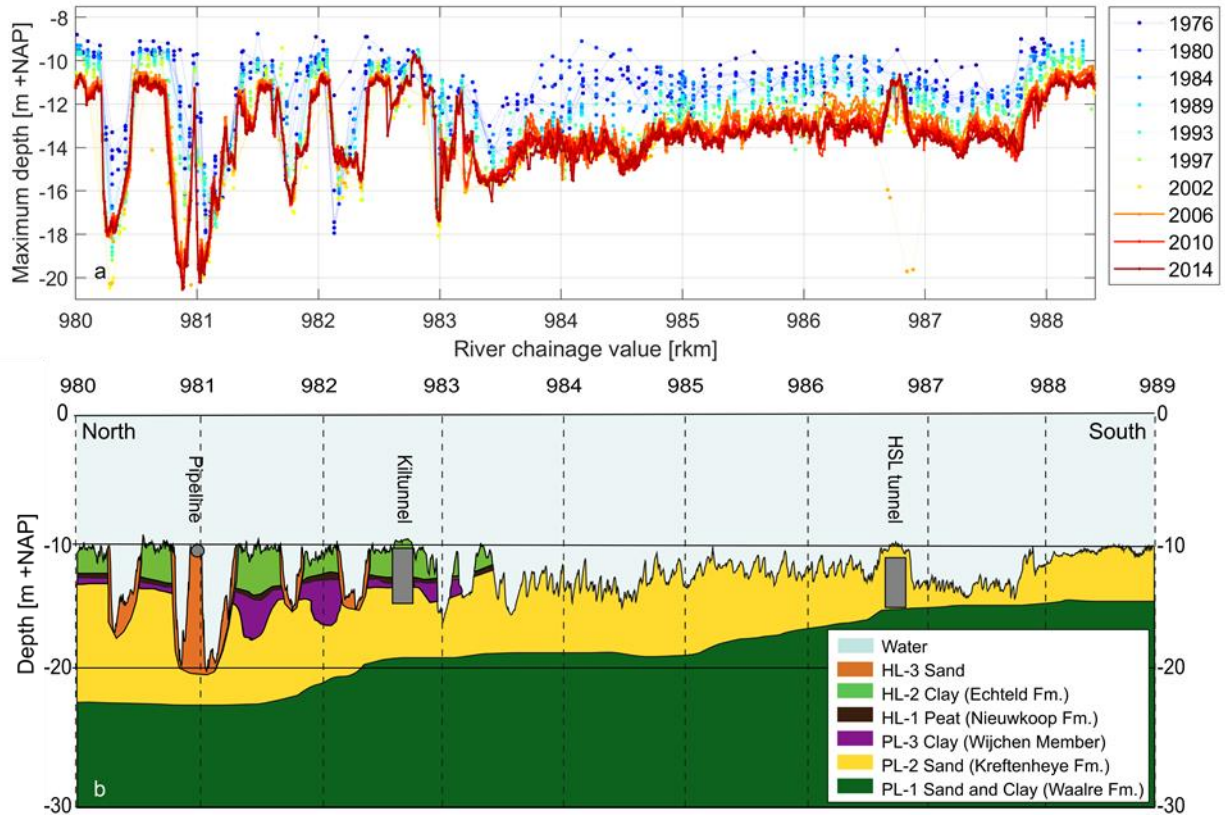
263 *Figure 4 a) overview of the bed level trends 2002-2012 from Becker (2015) and the identified scour holes (Huismans*
 264 *et al., 2016) of the Rhine-Meuse Estuary. b-c) 5-year scour hole growth in depth (left) and extent (right). d) Bar plot*
 265 *of the growth rates per region, namely southern branches (Merwedees, Bergsche Maas, Amer, Haringvliet, Hollandsch*
 266 *Diep), connecting branches (Spui, Oude Maas, Dordtsche Kil and Noord) and northern branches (Maasmond, Nieuwe*
 267 *Waterweg, Nieuwe Maas, Hollandsche IJssel and Lek). Maps are created in QGIS with the Esri-Grey (light) base*
 268 *map.*

269 The scour holes in the southern branches (Merwedees, Bergsche Maas, Amer, Haringvliet,
 270 Hollandsch Diep) show the smallest growth. The strongest growth is found in the connecting (Spui,
 271 Oude Maas, Dordtsche Kil and Noord) and northern channels (Maasmond, Nieuwe Waterweg,

272 Nieuwe Maas, Hollandsche IJssel and Lek). Note that without dredging the northern branches
273 would on average show aggradation instead of degradation. This means that the strongest scour
274 hole growth is not necessarily found in the branches with the highest erosion rate.

275 4.2 Scour hole formation in the eroding branches

276 To understand how the subsurface lithology controls bed degradation and scour hole
277 development, the bed level evolution from 1976 to 2015 is studied for two eroding branches, the
278 Dordtsche Kil and Oude Maas. Figure 5 shows the development of bed elevation in time of the
279 Dordtsche Kil. In four decades, several meters of erosion have occurred. There is a distinct
280 difference between the northern part (between river chainage value rkm 980 – 983) and the
281 southern part (rkm 983 – 989) of the river. In the southern part, the river bed eroded rather
282 homogeneously. In the northern part, the erosion is less and spread unevenly. This coincides with
283 the composition of the subsurface lithology, which in the southern part is homogeneous, consisting
284 of Pleistocene sand, allowing for homogeneous erosion. The subsurface lithology in the northern
285 part is heterogeneous and composed of poorly erodible clay interspersed with highly erodible sand
286 bodies from old channel belts. At locations where the river bed is composed of clay, erosion rates
287 are suppressed, while in the highly erodible sand patches, scour holes have emerged or existing
288 scour holes have undergone further erosion.



289

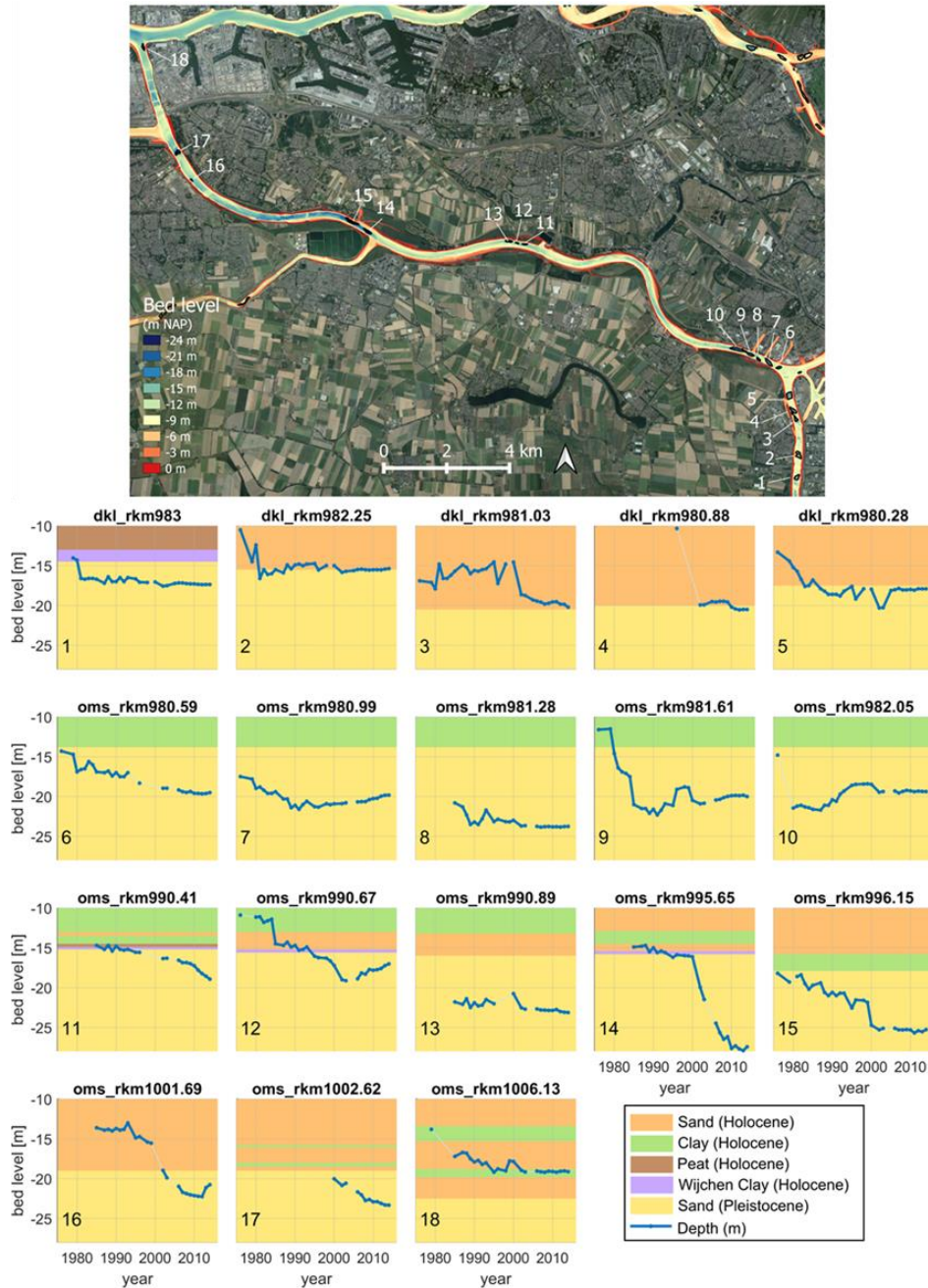
290 *Figure 5 a) evolution of the deepest points in the Dordtsche Kil river bed from 1976 to 2014. b) lithological*
 291 *longitudinal section of the Dordtsche Kil (Wiersma, 2015).*

292 For 18 scour holes in the Oude Maas and Dordtsche Kil river, the evolution of the scour
 293 hole depth is analysed for the period 1976 – 2014 (Figure 6). All scour holes have been subject to
 294 the same change in trend, namely an increase in flow velocities and resulting transport gradient
 295 due to closure of the Haringvliet. All scour holes have consequently grown in depth. The net
 296 increase in depth however strongly varies per scour hole. The largest net increase observed is 13
 297 m, which occurred in 35 years (scour hole 14, Figure 6), the smallest net increase is approximately
 298 1 m, which occurred in 29 years (scour hole 13). The rate at which the depth changes strongly
 299 varies as well. Some scour holes show a more gradual growth, others show clear trend breaks. In
 300 addition, the timing of acceleration or deceleration in growth is different for each scour hole.

301 Recent rates of depth change are generally lower than the overall growth rates. For 14 out of the
302 18 scour holes the average growth rate over the last five years is less than the average growth rate
303 over the total period. Five scour holes even show net sedimentation instead of erosion. This
304 suggests that most of the scour holes reached an equilibrium depth or are close to reaching this.
305 The exception may be scour hole 12, for which the timing of sedimentation coincides with an
306 increase in erosion of the neighbouring scour hole 11. As the tidal averaged flow is directed from
307 scour hole 11 to 12, this suggests that sedimentation in scour hole 12 is caused by an increase in
308 sediment availability from scour hole 11.

309 To get an indication on whether changes in growth rate can be related to the composition
310 of the subsurface lithology, the interpretation of the local subsurface lithology has been presented
311 in the coloured graphs. For the Oude Maas the interpretation was based on limited data
312 (Stouthamer & De Haas, 2011), and at some scour hole locations no interpretation could be made
313 due to lack of data. For these scour holes, either the closest subsurface lithology is taken as an
314 indication (scour holes 6-9, 11, 14, 15 and 16, data on average available within 800 m from the
315 scour hole location), or an interpolation of the closest by subsurface lithology is taken (scour holes
316 12 and 13).

317



318

319 *Figure 6 Top panel: map with scour hole locations considered for this analysis. Bed level is from 2014. Map is created*
 320 *in QGIS with the Esri-Satellite base map. Bottom panel: scour hole evolution over four decades. For each scour hole*
 321 *the evolution of the deepest point is shown in blue. In colour the subsurface lithology is presented. For the locations*
 322 *for which no subsurface lithology interpretation is available, either the closest by subsurface lithology is taken (scour*
 323 *holes 6-9, 11, 14, 15, 16, data on average available within 800 m from the scour hole location), or an interpolation*
 324 *of the closest by subsurface lithology is taken (scour holes 12 and 13).*

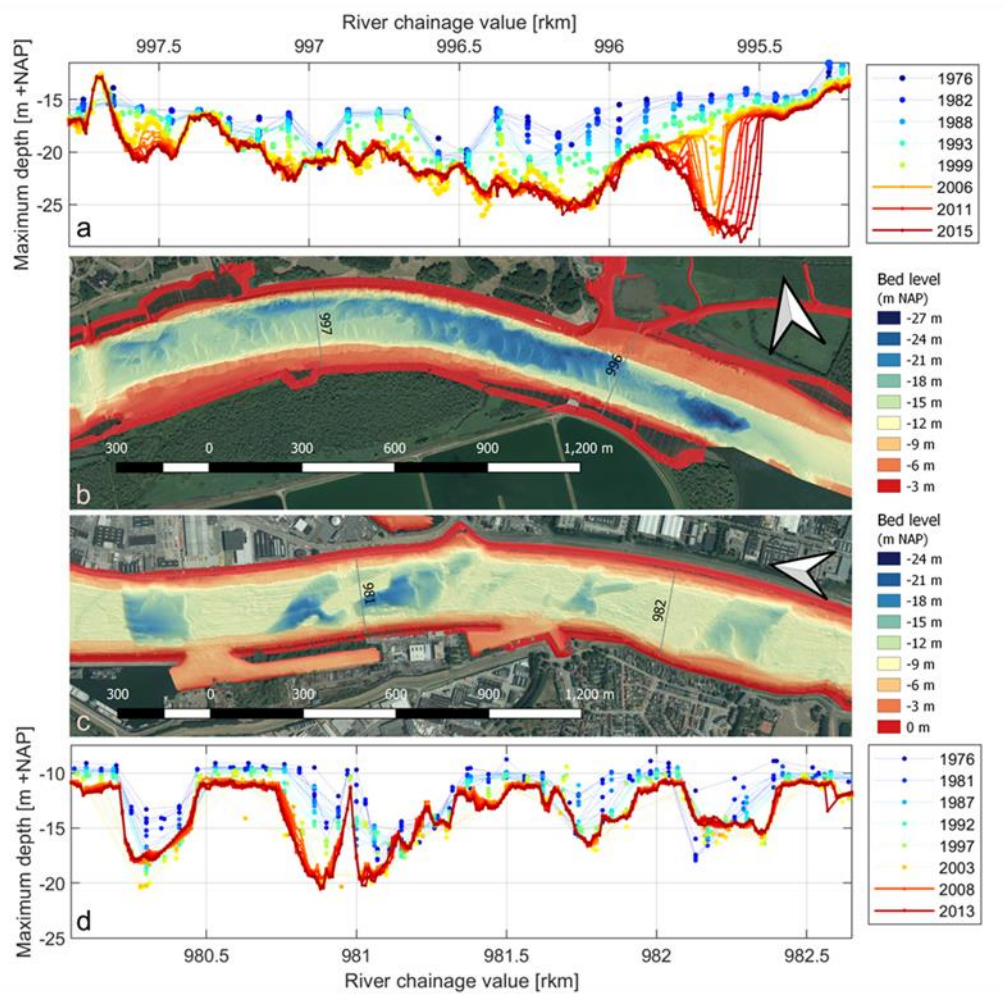
325 The graphs show that for scour holes 1, 9, 10, 12 14 and 18, the increase in growth rate
326 corresponds with a transition to a layer with a higher erodibility. For scour holes 2, 4, 5 and 18, a
327 decrease in growth rate coincides with a transition to a layer with lower erodibility. For some scour
328 holes (11, 15 and 16), the increase in growth rate cannot directly be related to changes in
329 erodibility. For scour holes 11 and 15, the transition to faster growth happens at larger depth than
330 the transition from clay to Pleistocene sand. As no interventions are known that can explain the
331 increase in growth rate, it is likely that locally the clay to sand transition is lower than suggested
332 by the lithological longitudinal section. For scour hole 16 the depth at which the growth rate
333 increases is in the middle of a sand layer. The nearby subsurface lithology is however very
334 heterogeneous. Within 1 km a clay layer is present at -16 m NAP, exactly the depth at which the
335 growth rate increased. This gives a strong indication that the transition to a faster growth is induced
336 by a transition from clay to sand.

337 4.3 Detailed growth in relation to the subsurface lithology

338 To estimate the risk of scour holes on the stability of nearby structures and river banks,
339 predictions on the scour hole growth rate and direction are required. For this purpose, three river
340 sections with scour holes of distinct size, shape, growth rate and direction are analysed in relation
341 to their subsurface lithology.

342 In Figure 7, the present bed level and evolution of the deepest points along the river (1976-
343 2015) are shown for a 2 km river section of the Oude Maas and Dordtsche Kil. The bed topography
344 of the Oude Maas section shows an elongated scour hole of over 1 km length and two smaller ones
345 at rkm 995.7 and 997.5. The evolution of the deepest points indicates that the elongated scour hole
346 initially consisted of two or three scour holes which developed in depth and extent and merged
347 together. Both smaller scour holes are not present in the 1976 surveys and only emerge around

348 2000 and 2005 for respectively the scour hole at rkm 997.5 and 995.7. The scour hole at rkm 995.7
 349 is extending mostly in eastward direction but also westward, in the direction of the elongated scour
 350 hole. If this trend continues, this scour hole will merge with the elongated scour hole to form an
 351 even larger one.

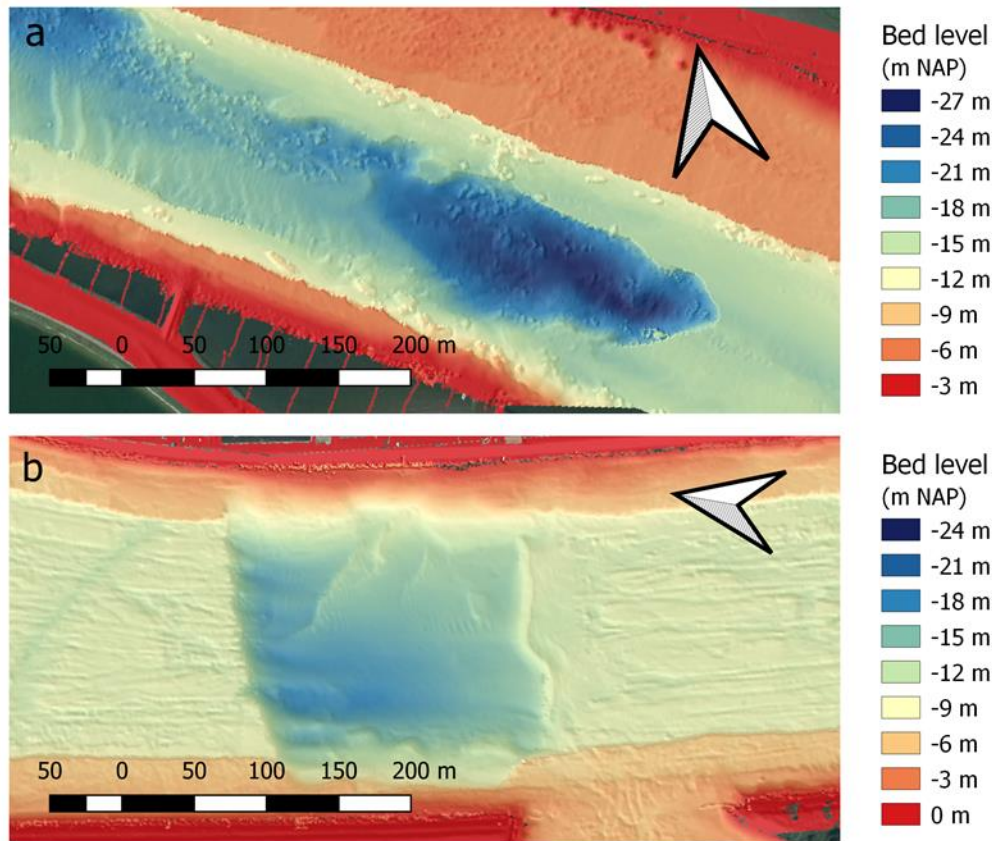


352

353 *Figure 7 Detailed scour hole evolution for two locations. a) Evolution of the deepest points in the Oude Maas (rkm*
 354 *997.25 – 995.75), b) corresponding bed topography in 2014. Residual or net sediment-transport direction is westward*
 355 *(to the left in the figure). c) Bed topography Dordtsche Kil (rkm 980.1 – 982.6) in 2014 and d) corresponding evolution*
 356 *of the deepest points. The residual or net sediment-transport direction is northward (to the left in the figure). Maps*
 357 *are created in QGIS with the Esri-Satellite base map.*

358 The scour hole size, growth and shape observed in the displayed section of the Dordtsche
359 Kil, are very different from the scour holes in the Oude Maas section. The scour holes are smaller,
360 with a length of about 200 to 300 m and are irregularly shaped, with seemingly artificial shapes
361 containing sharp angles and rectangular like features. None of the scour holes merged, nor trends
362 are observed which suggest that scour holes will merge. Over the last 8 years, the scour holes show
363 only minor evolution.

364 A close up of the bed topography around Oude Maas rkm 995.7 and Dordtsche Kil rkm
365 980.2 is given in Figure 8. The bed topography east of the scour hole in the Oude Maas
366 (rkm < 995.5, bed elevation around NAP -16 m) is very smooth, suggesting the presence of a clay
367 layer, which prevents the formation of bed forms. Nearby core descriptions indicate this is likely
368 clay from the Wijchen Mb., which is found to be present at an elevation of about NAP -16 m (see
369 also the subsurface lithology at rkm 995.65 in Figure 6). In and westward of the scour hole, big
370 blocks of material are observed, which are hypothesized to be blocks of clay that crumbled from
371 the edges in response to undermining of the clay layer by the force of the flow. The bed topography
372 around the scour hole in the Dordtsche Kil shows elongated scratches. Distinct scratches from
373 dredging activities and shipping scours indicate a resistant soil type in which marks do not easily
374 smooth or vanish, likely clay. The subsurface lithological longitudinal section supports this
375 hypothesis.



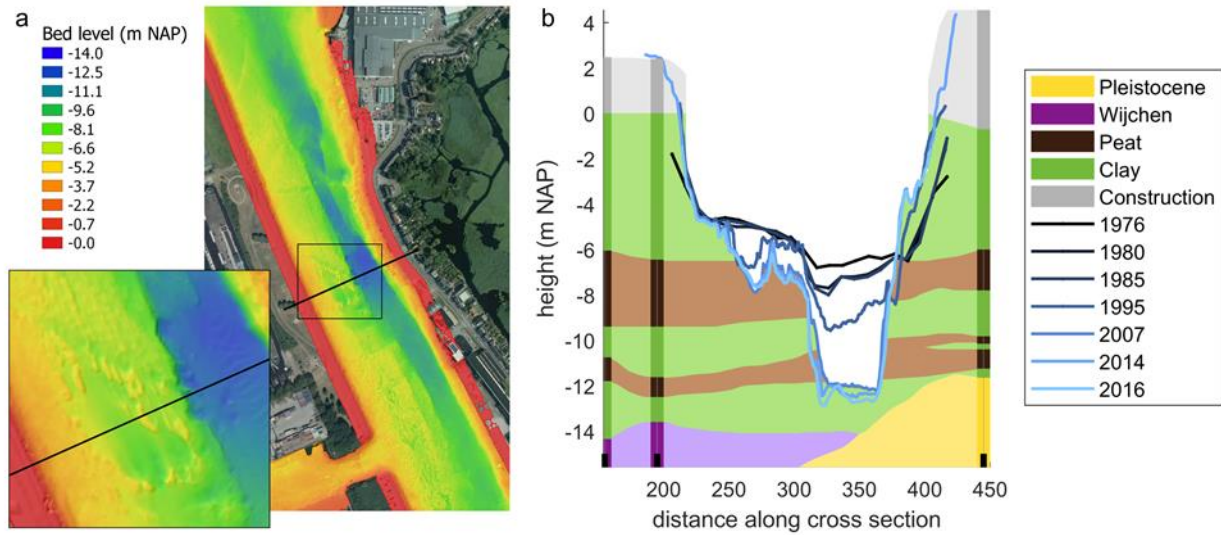
376

377 *Figure 8 a) Bed topography of the scour hole in the Oude Maas at rkm 995.7 b) and of the scour hole in the*
 378 *Dordtsche Kil at 980.2, both 2014. The smooth bed in the top figure is attributed to a clay layer. The blocks of*
 379 *material in- and downstream of the scour hole are hypothesized to be blocks of clay that crumbled off the edges. The*
 380 *scratches in the bottom figure are attributed to the occurrence of a resistant soil type, likely clay. They do not show*
 381 *a development over time. Maps are created in QGIS with the Esri-Satellite base map.*

382 Based on these observations, the difference in shape and opposite trends in scour hole
 383 evolution in the displayed Oude Maas and Dordtsche Kil reach, can be related to the subsurface
 384 lithology. The scour holes in the Oude Maas are formed by abrasion of the clay layer and ultimately
 385 breaching through of this layer, such that the underlying Pleistocene sand gets exposed to the flow.
 386 The edges of the scour holes consist of a relatively thin layer of clay (1 to 2 m), which is thin
 387 enough to get crumbled at the edges (Figure 8). As a result, scour holes develop both in depth and
 388 area and eventually merge. The Dordtsche Kil scour holes are formed in the sandy channel-belt

389 sand bodies that are crossed by the current river course. According to the lithological longitudinal
390 section in Figure 5, the subsurface flanking the channel-belt sand bodies consists of thick layers
391 of poorly erodible peat and clay with a varying thickness of 3 to 8 meter, suppressing erosion in
392 lateral direction and confining the scour holes to the size of the channel belt. This may also explain
393 the typical rectangular like shape of some of the scour holes, as the current river channel crosses
394 the channel-belt sand bodies. The sharp edges observed may be related to outcrops of peat. Though
395 the thick peat layer currently confines the scour holes to the area of the channel belt, slopes within
396 the scour holes are observed to slowly get steeper, indicating that growth has not stopped entirely.

397 The third in detail investigated location is in the Noord River (Figure 9). At this location
398 an elongated scour hole developed at the eastern side of the river. The evolution of the cross
399 sections shows a slight asymmetry already present in 1976. Between 1976 and 2016, 0 to 2 m
400 erosion occurred in depth at the western side, while up to 6 m erosion occurred at the eastern side,
401 leading to a total asymmetry of about 6 m. At the western side the bed topography displays
402 irregular features that show up as small yellow patches in the top view presented in Figure 9a and
403 oscillations in the cross sections in Figure 9b. Core descriptions also indicate an asymmetry in the
404 subsurface lithology, with a thicker layer of peat at the western side and deep down at
405 about -14 m NAP erosion resistant Wijchen Mb. clay and a thinner layer of peat on the eastern
406 side and deep down at about -12 m NAP Pleistocene sand.



407

408 *Figure 9 a) bed topography of a scour hole in the Noord (2014). Map is created in QGIS with the Esri-Satellite base*
 409 *map. b) evolution of the river bed at several moments in time, superposed on a reconstruction of the subsurface*
 410 *lithology (Stouthamer & De Haas, 2011). Boreholes are shown in bright colour; the interpolation is shown in faded*
 411 *colour.*

412 As the river narrows locally, the river bed is expected to be deeper at this location. The
 413 strong asymmetric development is hypothesized to be an interplay between asymmetries in both
 414 the hydrodynamic conditions and in the subsurface lithology. The initial asymmetry, as observed
 415 in 1976, is likely caused by asymmetric flow patterns induced by the local channel narrowing at
 416 the eastern side of the channel. The observed irregularities on the western part are attributed to the
 417 presence of peat, showing that this part of the river is located in a poorly erodible peat layer which
 418 is only slowly degrading. Due to the asymmetry in the flow, the eastern side of the channel
 419 succeeded to completely erode this poorly erodible peat layer and reached its base at around 1995.
 420 Since then the erosion accelerated, as it reached the underlying clay layer, which generally has a
 421 higher erodibility, especially when some sand is mixed. This has further enhanced the asymmetric
 422 development.

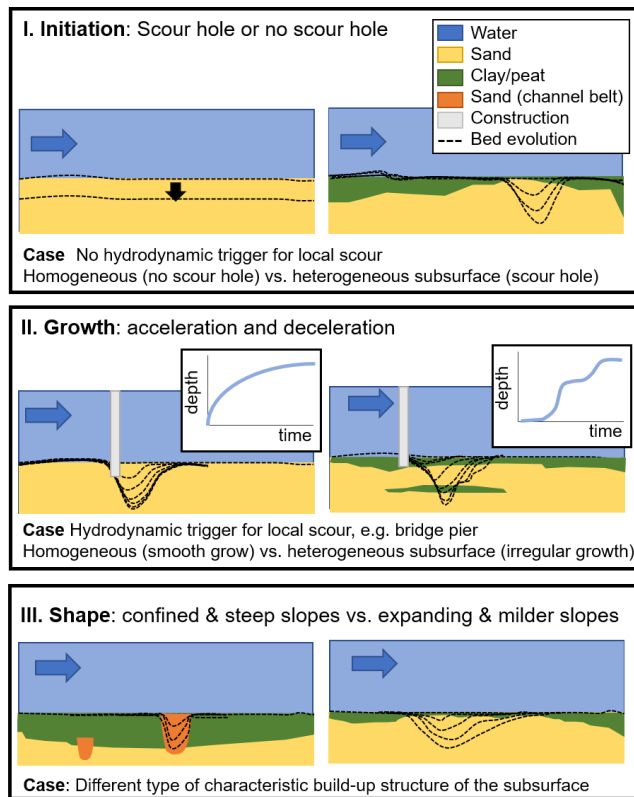
423 To confirm this hypothesis, new corings should be carried out. These could also shed light
424 on the recent evolution of the scour hole. Since 2007 the scour hole is only slowly growing in
425 depth. This suggests that the peat layer that is interpreted to be located at about -10 to -11 m NAP,
426 may actually be located a bit deeper, at about -12 m NAP, as is the case on the western side of the
427 channel (see borehole data in Figure 9). This would then match the observation of a fast growth
428 between -9 m NAP (1995) and -12 m NAP (2007) and the limited growth since then.

429 **5 Discussion**

430 5.1 Lithological control on scour hole formation

431 Most prominent from the analysis is the diversity of the size, shape and growth
432 characteristics of the scour holes. Various factors likely contribute. Firstly, the causes that trigger
433 scour hole formation range from bend scour (e.g. Andrieu, 1994; Beltaos et al., 2011; Blanckaert,
434 2010; Engelund, 1974; Gharabaghi et al., 2007; Odgaard, 1981; Ottevanger et al., 2012;
435 Vermeulen et al., 2015; Zimmermann & Kennedy, 1978), confluence scour (e.g. Best, 1986; Best
436 & Rhoads, 2008; Ferrarin et al., 2018; Silvia S. Ginsberg & Perillo, 1999; Ginsberg et al., 2009;
437 Kjerfve et al., 1979; Mosley, 1976; Pierini et al., 2005), local channel narrowing and local scour
438 induced by the impact of a structure on the flow, like bridge piers, groynes and bed protection (e.g.
439 Liang et al., 2020; Pandey et al., 2018; Wang et al., 2017). These types of scour holes evolve
440 differently, have different shapes and as a result different relations for predicting their equilibrium
441 depth (Hoffmans & Verheij, 1997). Secondly, conditions like flow velocity, water depth and grain
442 size that influence scour hole growth, vary throughout the estuary. Third reason is the lithological
443 influence on scour hole formation, which in current analyses proves to be a major influence on
444 scour hole initiation, growth rate and shape and which in certain cases even overrules the above
445 listed causes and controls. In figure 10 the three lithological controls are illustrated.

446 Firstly, lithology may trigger scour hole formation (Fig. 10a). A prominent example is the
447 large-scale incision of the Dordtsche Kil river into the heterogeneous subsurface lithology, leading
448 to formation of scour holes of up to two times the average water depth at locations with higher
449 erodibility. At these locations no other causes for scour hole formation are present. In the southern
450 part, where the river incises into a homogeneous sand layer, no scour holes are found, while the
451 hydrodynamic conditions are similar. This forms the most direct proof that variations in lithology
452 cause scour hole formation. It is in line with observations by Cserkés-Nagy et al. (2010), who
453 reasoned scour holes observed in a straight river section to be triggered by variations in the
454 subsurface lithology and with Sloff et al. (2013) who demonstrated this process conceptually and
455 numerically. Secondly, lithology determines whether and when a scour hole can form and when
456 fluctuations in growth rate occur (Fig. 10b). An insightful example is the scour hole at the
457 confluence of the Spui and Oude Maas river (Figs. 6-7). Though the confluence in its present
458 outline already exists for over a century (www.topotijdreis.nl), no confluence scour emerged until
459 recently in 2005. Only after reaching a transition from resistant clay to sand, in ten years' time a
460 scour hole with a depth of -27 m NAP emerged, i.e. an average growth in depth of 11 m in 10 year.
461 These abrupt changes in growth in depth are observed for various scour holes in the Rhine-Meuse
462 Estuary (Figure 6) and can in most cases be related to a transition in lithology with different
463 erodibility. Though not proven, it is also the most likely cause for abrupt changes in growth for
464 the other scour holes, as other causes like a strong increase in flow, a newly placed construction,
465 or failure of bed protection do not apply.



466

467 *Figure 10. Summary of the observed lithological controls on scour hole development. All figures display a longitudinal*
 468 *section of a river reach, with the blue arrow indicating the flow direction. Dashed lines represent the bed level*
 469 *development over time.*

470 Thirdly, in horizontal direction the subsurface lithology can be a dominant factor in
 471 determining the shape or growth rate (Fig. 10c). Scour holes with edges composed of thin layers
 472 of clay (< 2 m thickness), are observed to grow in extent. In high resolution multibeam surveys,
 473 indications are found that these clay layers are undermined and crumble, enabling the scour hole
 474 to grow laterally and merge with nearby scour holes. As a resultant scour holes form of more than
 475 a kilometre in length. The opposite is observed for the scour holes in the Dortdsche Kil, which are
 476 relatively small (< 300 m in length) and show only subtle changes in horizontal direction. These
 477 scour holes are formed in former channel belts and their edges consist of thick layers of peat and

478 clay (3 to 8 m thickness), confining the scour holes to the extent of the channel belt, suppressing
479 further growth in extent.

480 In case of variations in subsurface lithology over the river cross section, scour holes can
481 take an asymmetric shape and get confined to only one side of the channel. In this case, there may
482 be an extra positive feedback with the flow. In the deeper part flow attraction may occur, with
483 higher relative flow velocities with respect to the shallower part of the cross section (Sloff et al.,
484 2013), as a result of lower relative friction. Due to the enhanced relative flow velocities, shear
485 stresses at the deeper part of the river bed are higher than at the sides, which further enhances the
486 asymmetry in erosion.

487 The strong lithological control on scour hole formation is in line with the reported effect
488 of the subsurface lithology on the formation of eb-tidal channels in the Ems (Pierik et al., 2019)
489 and erosion and lateral migration of the Tisza river (Cserkész-Nagy et al., 2010). It may also
490 explain the deviations in expected scour depth, location and shape observed in the Venice Lagoon
491 (Ferrarin et al., 2018).

492

493 5.2 Equilibrium

494 There is no clear relation between recent 5-year scour hole growth and overall bed level
495 degradation. This means that the strongest scour hole growth is not necessarily found in the
496 branches with the highest erosion rate. The occurrence of local scour and sand mining may explain
497 some of these cases, but a closer look at the 40-year depth evolution of the scour holes in the
498 eroding Dordtsche Kil and Oude Maas branches shows that for most of the scour holes, the recent
499 depth growth rates have decreased or even reversed to sedimentation. In response to the higher

500 flow velocities due to closure of the Haringvliet, the scour hole depth increased for all cases. As
501 Haringvliet was closed decades ago, it is likely that most scour holes are reaching an equilibrium
502 depth, like also occurs for local scour induced by constructions (Hoffmans & Verheij, 1997). That
503 an equilibrium depth also applies for the scour holes induced or influenced by a heterogeneous
504 subsurface lithology is plausible, as the same physics apply. The deeper the scour hole gets, the
505 more effort it takes to transport sediment up the slope while, depending on how the flow structures
506 evolve, generally the flow velocities within the scour hole decrease with depth. Another
507 explanation for a slower or reversed depth development may be the presence of a poorly erodible
508 layer at the bottom of the scour hole (Cserkés-Nagy et al., 2010). This is clearly the case for scour
509 hole 18 (Figure 18), which reached a poorly erodible clay layer. It may also be a factor for the
510 scour holes in the Dordtsche Kil, as the depth of the channel-belt sand bodies in which the scour
511 holes formed is interpreted to be close to the current scour hole depth (Figure 5). As the channel-
512 belt bodies are commonly composed of finer grained sands than the coarser grained Pleistocene
513 sand layer below (e.g. Berendsen, 1982; Gouw & Erkens, 2007; Weerts & Busschers, 2003), the
514 erodibility is lower, reducing the scour hole depth growth. According to the lithological
515 longitudinal sections, most of the Oude Maas scour holes are already based within the Pleistocene
516 sand and are not at a depth close to reaching a transition in lithological composition. However, as
517 the Pleistocene sand gradually coarsens with depth (Busschers et al., 2005, 2007), this may still
518 have an impact. For these scour holes, it is likely that a combination of coarsening of sediment
519 with reduced hydraulic forcing due to reaching a larger depth, results in a reduced growth or
520 stabilization of depth. To further quantify the relative contributions of each process a combination
521 of flow measurements and calculations with data on the grainsize distribution in the lower part of
522 the scour hole is needed.

523 5.3 Consequences and risks for other rivers and estuaries

524 Provided enough hydraulic forcing, the subsurface lithology can have a large impact on
525 when and where scour holes form, or even be dominant. The observed influences and controls on
526 initiation, growth rates and size, as illustrated in Figure 10, apply to any system with a
527 heterogeneous substratum of alternating peat, clay and sand deposits. Though little has been
528 reported, these controls are therefore likely not unique to the Rhine-Meuse Estuary. Channel bed
529 degradation, also occurs in other large delta rivers like the Yangtze, the Mississippi and the
530 Mekong (Brunier et al., 2014; Galler et al., 2003; Hoitink et al., 2017; Luan et al., 2016; Sloff et
531 al., 2013; B. Wang & Xu, 2018). And as causes are mainly anthropogenic, more delta rivers are
532 expected to follow. Given the fact that river deltas commonly have a heterogeneous substratum of
533 alternating peat, clay and sand deposits (e.g. Aslan & Autin, 1999; Aslan et al., 2005; Berendsen
534 & Stouthamer, 2001, 2002; Cohen et al., 2012; Gouw & Autin, 2008; Hanebuth et al., 2012; Kuehl
535 et al., 2005.; Stefani & Vincenzi, 2005), scour hole formation in heterogeneous subsurface is
536 expected to become a problem in more deltas. Hints are there that for the Ems river (Pierik et al.
537 2019), the Venice Lagoon (Ferrarin et al., 2018), Mississippi river (Nittrouer et al., 2011) and the
538 Mekong river, the subsurface lithology already plays a role in the scour hole development, as scour
539 holes in these studies show deviating location, shape or depth, while the subsurface is
540 heterogeneous. When for these systems only the hydraulic component is taken into account, as
541 commonly the case, there will be a misprediction of the scour hole evolution, depth, shape and
542 location. In case scour holes are close to infrastructure or river banks, stability is at stake. As
543 accurate predictions on scour hole formation are of high importance, especially in densely
544 occupied areas like deltas (Best, 2019; Syvitski et al., 2009), we therefore advocate to explicitly
545 include the geology, when predicting scour hole formation and growth. This requires knowledge

546 of the subsurface lithology, acquired with a combination of measurements and geological
547 interpretation, as elaborated in the methods section. Based on the specific geological structure, the
548 risk of new scour hole formation can be assessed, as well as the likelihood whether scour holes
549 stay confined or expand. Given the other controls of lithology on the lateral behaviour of river
550 branches (Cserkés-Nagy et al., 2010) and the evolution of eb-flood channels (Pierik et al., 2019),
551 it is important to include the lithology into numerical models (van der Wegen & Roelvink, 2012).
552 Therefore, measuring subsurface lithology and including these parameters in scour-hole risk-
553 assessments and numerical models will be an important improvement over current analysis, which
554 focus mainly on the hydraulic forcing assuming a homogenous substrate.

555

556 **6 Conclusions**

557 Although a vast amount of research has been carried out on scour holes, little is known on
558 how the lithology influences the location, size, shape and growth rates of scour holes. This is,
559 however, essential information in judging whether scour holes form a risk for the stability of river
560 banks, dikes or other nearby infrastructure. The present study presents a first in depth analysis on
561 how the lithology controls the bed topography and scour hole growth in particular. The Rhine-
562 Meuse estuary is used as a study area, as over 100 scour holes are present and detailed data are
563 available on both bed level evolution and subsurface lithological composition.

564 From analysing over 40 years of bed level evolution in relation to the geology, it is shown
565 that subsurface lithology can play a crucial role in the emergence of scour holes, their shape and
566 evolution. In the Rhine-Meuse Estuary several branches are eroding in response to closure of one
567 of its tidal outlets. Reaches with a sandy subsurface erode evenly, while in reaches with a

568 heterogeneous subsurface lithology erosion is retarded at locations with a poorly erodible top layer
569 and promoted at locations where locally a sandy subsurface is present. At these locations, deep
570 scour holes form with depths of up to two times the average water depth. Their shapes can be very
571 irregular and strongly deviating from an oval like shape. These shapes are imposed by the poorly
572 erodible top layer, inhibiting the scour hole to more naturally grow in width or length. The
573 consequent growth characteristics are often erratic, with sudden changes in depth or extent.
574 Naturally, scour holes follow an exponential development with a fast initial growth and slower
575 final growth. Though this analysis shows that scour holes in heterogeneous subsurface generally
576 follow the same growth curve, temporally strong variations in development in depth or extent are
577 observed.

578 The direction of growth is also strongly determined by the composition of the subsurface.
579 Scour holes with edges composed of thin layers of clay are observed to grow in extent. Indications
580 are found that the thin clay layers crumble and enable scour holes to grow laterally and merge with
581 nearby scour holes, forming elongated scour holes of more than a kilometre in length. The opposite
582 is observed for scour holes that are formed in channel belts with thick peat and clay layers at their
583 edges, confining the scour holes to the extent of the channel-belt sand body crossed by the river
584 channel and allowing for limited growth in horizontal direction. In case of asymmetries in the
585 erodibility over the channel width, scour holes take an asymmetric shape and can get confined to
586 only one side of the channel, nearing a channel bank.

587 These findings emphasize the crucial role that geology plays in the spatial and temporal
588 evolution of river bed erosion. It co-determines the pace of erosion and the related long-term
589 evolution of river branches and tidal channels and it can initiate and influence scour hole formation.
590 It therefore calls for good knowledge of the subsurface lithology as without, the erratic scour hole

591 development is hard to predict and can lead to sudden failures of nearby infrastructure and flood
592 defence works. In addition, for making proper morphodynamic predictions, information on the
593 subsurface lithology needs to be included in numerical models.

594 **Data Availability Statement**

595 There is no restriction on the data used in this study. Bed topography data can be requested at
596 Rijkswaterstaat via [https://www.rijkswaterstaat.nl/formulieren/contactformulier-servicedesk-](https://www.rijkswaterstaat.nl/formulieren/contactformulier-servicedesk-data.aspx)
597 [data.aspx](https://www.rijkswaterstaat.nl/formulieren/contactformulier-servicedesk-data.aspx). Lithological core descriptions can be downloaded from the DINO loket:
598 www.dinoloket.nl. Lithological sections constructed from the lithological core descriptions are
599 available in (Huisman et al., 2013; Stouthamer & De Haas, 2011; Stouthamer et al., 2011b-d;
600 Wiersma, 2015). Channel belt reconstruction can be downloaded from
601 <http://dx.doi.org/10.17026/dans-x7g-sjtw> (Cohen et al., 2012).

602 **Acknowledgments**

603 The research presented in this paper builds on several projects initiated and funded by
604 Rijkswaterstaat (RWS). This study was furthermore funded by Deltares Research Funds. We
605 greatly acknowledge efforts from Aad Fioole (RWS) on the data handling and sharing and value
606 the discussions with Arjan Sieben (RWS), Pim Neefjes (RWS) and Arie Broekhuizen (RWS).

607

608 **References**

609 Andrie, R. (1994). Flow structure and development of circular meander pools. *Geomorphology*, 9(4), 261–270.
610 [https://doi.org/10.1016/0169-555X\(94\)90049-3](https://doi.org/10.1016/0169-555X(94)90049-3)

611 Aslan, A., & Autin, W. J. (1999). Evolution of the Holocene Mississippi River floodplain, Ferriday, Louisiana;
612 insights on the origin of fine-grained floodplains. *Journal of Sedimentary Research*, 69(4), 800–815.
613 <https://doi.org/10.2110/jsr.69.800>

614 Aslan, A., Autin, W. J., & Blum, M. D. (2005). Causes of River Avulsion: Insights from the Late Holocene
615 Avulsion History of the Mississippi River, U.S.A. *Journal of Sedimentary Research*, 75(4), 650–664.
616 <https://doi.org/10.2110/jsr.2005.053>

617 Becker, A. (2015). *Sediment in (be)weging, deel 2 (periode 2000-2012). English: Sediment budget of the Rhine*
618 *Meuse Estuary (2000-2012)* (No. 1208925-000-ZWS-0023). Delft, the Netherlands: Deltares.

619 Beltaos, S., Carter, T., & Prowse, T. (2011). Morphology and genesis of deep scour holes in the Mackenzie Delta.
620 *Canadian Journal of Civil Engineering*, 38(6), 638–649. <https://doi.org/10.1139/111-034>

621 Berendsen, Henk J.A., & Stouthamer, E. (2000). Late Weichselian and Holocene palaeogeography of the Rhine–
622 Meuse delta, The Netherlands. *Palaeogeography, Palaeoclimatology, Palaeoecology*, 161(3), 311–335.
623 [https://doi.org/10.1016/S0031-0182\(00\)00073-0](https://doi.org/10.1016/S0031-0182(00)00073-0)

624 Berendsen, H.J.A. (1982). *De genese van het landschap in het zuiden van de provincie Utrecht, een fysisch-
625 geografische studie*. (PhD-thesis). Utrecht University, Utrecht, the Netherlands.

626 Berendsen, H.J.A., Hoek, W. Z., & Schorn, E. A. (1995). Late Weichselian and Holocene river channel changes of
627 the rivers Rhine and Meuse in the central Netherlands (Land van Maas en Waal). In *European river activity
628 and climate change during the Lateglacial and Early Holocene. ESF Project European
629 Paläoklimaforschung / Paleoclimate Research, Special Issue* (pp. 151–171). Frenzel, B. (ed.).

630 Berendsen, H.J.A., & Stouthamer, E. (2001). *Paleogeographic development of the Rhine-Meuse delta, The
631 Netherlands* (1st printing). Assen: Koninklijke Van Gorcum.

632 Berendsen, H.J.A., & Stouthamer, E. (2002). Paleogeographic evolution and avulsion history of the Holocene
633 Rhine-Meuse delta, The Netherlands. *Netherlands Journal of Geosciences - Geologie En Mijnbouw*, 81(1),
634 97–112. Cambridge Core. <https://doi.org/10.1017/S0016774600020606>

635 Best, J. L. (1986). The morphology of river channel confluences. *Progress in Physical Geography: Earth and
636 Environment*, 10(2), 157–174. <https://doi.org/10.1177/030913338601000201>

637 Best, J. L., & Rhoads, B. L. (2008). Sediment transport, bed morphology and the sedimentology of river channel
638 confluences. In *River confluences, tributaries and the fluvial network* (pp. 45–72). Chichester, UK: In S. P.
639 Rice, A. G. Roy, & B. L. Rhoads (Eds.) John Wiley & Sons, Ltd.

640 Blanckaert, K. (2010). Topographic steering, flow recirculation, velocity redistribution, and bed topography in sharp
641 meander bends. *Water Resources Research*, 46(9). <https://doi.org/10.1029/2009WR008303>

642 Brunier, G., Anthony, E. J., Goichot, M., Provansal, M., & Dussouillez, P. (2014). Recent morphological changes in
643 the Mekong and Bassac river channels, Mekong delta: The marked impact of river-bed mining and
644 implications for delta destabilisation. *Geomorphology*, 224, 177–191.
645 <https://doi.org/10.1016/j.geomorph.2014.07.009>

646 Busschers, F. S., Kasse, C., van Balen, R. T., Vandenberghe, J., Cohen, K. M., Weerts, H. J. T., ... Bunnik, F. P. M.
647 (2007). Late Pleistocene evolution of the Rhine-Meuse system in the southern North Sea basin: Imprints of
648 climate change, sea-level oscillation and glacio-isostasy. *Quaternary Science Reviews*, 26(25), 3216–3248.
649 <https://doi.org/10.1016/j.quascirev.2007.07.013>

650 Busschers, F. S., Weerts, H. J. T., Wallinga, J., Cleveringa-a2, P., Kasse, C., de Wolf, H., & Cohen, K. M. (2005).
651 Sedimentary architecture and optical dating of Middle and Late Pleistocene Rhine-Meuse deposits—Fluvial
652 response to climate change, sea-level fluctuation and glaciation. *Netherlands Journal of Geosciences -*
653 *Geologie En Mijnbouw*, 84(1), 25–41. Cambridge Core. <https://doi.org/10.1017/S0016774600022885>

654 Cohen, K. M. (2003). *Differential subsidence within a coastal prism: Late-Glacial—Holocene tectonics In The*
655 *Rhine-Meuse delta, the Netherlands* (PhD-thesis). Utrecht University.

656 Cohen, K. M., Stouthamer, E., Pierik, H. J., & Geurts, A. H. (2012). *Digital Basemap for Delta Evolution and*
657 *Palaeogeography*. Utrecht University. DANS. Retrieved from <http://dx.doi.org/10.17026/dans-x7g-sjtw>

658 Cserkés-Nagy, Á., Tóth, T., Vajk, Ö., & Sztanó, O. (2010). Erosional scours and meander development in response
659 to river engineering: Middle Tisza region, Hungary. *Fluvial Records as Archives of Human Activity and*
660 *Environmental Change*, 121(2), 238–247. <https://doi.org/10.1016/j.pgeola.2009.12.002>

661 de Haas, T., Pierik, H. J., van der Spek, A. J. F., Cohen, K. M., van Maanen, B., & Kleinhans, M. G. (2018).
662 Holocene evolution of tidal systems in The Netherlands: Effects of rivers, coastal boundary conditions,
663 eco-engineering species, inherited relief and human interference. *Earth-Science Reviews*, 177, 139–163.
664 <https://doi.org/10.1016/j.earscirev.2017.10.006>

665 de Haas, Tjalling, van der Valk, L., Cohen, K. M., Pierik, H. J., Weisscher, S. A. H., Hijma, M. P., ... Kleinans, M.
666 G. (2019). Long-term evolution of the Old Rhine estuary: Unravelling effects of changing boundary
667 conditions and inherited landscape. *The Depositional Record*, 5(1), 84–108.
668 <https://doi.org/10.1002/dep2.56>

669 Englund, F. (1974). *Flow and bed topography in channel bends*. 100, 1631–1648.

670 Erkens, G. (2009). *Sediment dynamics in the Rhine catchment—Quantification of fluvial response to climate change
671 and human impact*. Utrecht University, Utrecht, the Netherlands.

672 Ferrarin, C., Madricardo, F., Rizzetto, F., Kiver, W. M., Bellafiore, D., Umgieser, G., ... Trincardi, F. (2018).
673 Geomorphology of Scour Holes at Tidal Channel Confluences. *Journal of Geophysical Research: Earth
674 Surface*, 123(6), 1386–1406. <https://doi.org/10.1029/2017JF004489>

675 Frings, R. M., Hillebrand, G., Gehres, N., Banhold, K., Schriever, S., & Hoffmann, T. (2019). From source to
676 mouth: Basin-scale morphodynamics of the Rhine River. *Earth-Science Reviews*, 196, 102830.
677 <https://doi.org/10.1016/j.earscirev.2019.04.002>

678 Fugro. (2002). *Laboratoriumresultaten betreffende morfologisch modelleren (datarapport)* (No. Opdracht-nummer
679 H-4086).

680 Galler, J. J., Bianchi, T. S., Alison, M. A., Wsocki, L. A., & Campanella, R. (2003). Biogeochemical implications
681 of levee confinement in the lowermost Mississippi River. *Eos, Transactions American Geophysical Union*,
682 84(44), 469–476. <https://doi.org/10.1029/2003EO440001>

683 Gharabaghi, B., Inkratas, C., Beltaos, S., & Krishnappan, B. (2007). Modelling of three-dimensional flow velocities
684 in a deep hole in the East Channel of the Mackenzie Delta, Northwest Territories. *Canadian Journal of
685 Civil Engineering*, 34(10), 1312–1323. <https://doi.org/10.1139/l07-054>

686 Ginsberg, S. S., & Perillo, G. M. E. (1999). Deep-scour holes at tidal channel junctions, Bahia Blanca Estuary,
687 Argentina. *Marine Geology*, 160(1), 171–182. [https://doi.org/10.1016/S0025-3227\(99\)00019-5](https://doi.org/10.1016/S0025-3227(99)00019-5)

688 Gouw, Marc J.P., & Autin, W. J. (2008). Alluvial architecture of the Holocene Lower Mississippi Valley (U.S.A.)
689 and a comparison with the Rhine–Meuse delta (The Netherlands). *Sedimentary Geology*, 204(3), 106–121.
690 <https://doi.org/10.1016/j.sedgeo.2008.01.003>

691 Gouw, M.J.P., & Erkens, G. (2007). Architecture of the Holocene Rhine-Meuse delta (the Netherlands)—A result of
692 changing external controls. *Netherlands Journal of Geosciences - Geologie En Mijnbouw*, 86(1), 23–54.
693 Cambridge Core. <https://doi.org/10.1017/S0016774600021302>

694 Hanebuth, T. J. J., Proske, U., Saito, Y., Nguyen, V. L., & Ta, T. K. O. (2012). Early growth stage of a large delta—
695 Transformation from estuarine-platform to deltaic-progradational conditions (the northeastern Mekong
696 River Delta, Vietnam). *Sedimentary Geology*, 261–262, 108–119.
697 <https://doi.org/10.1016/j.sedgeo.2012.03.014>

698 Hijma, M. P. (2009). *From river valley to estuary. The early-mid Holocene transgression of the Rhine-Meuse valley,*
699 *The Netherlands.* (PhD-thesis). KNAG/Faculty of Geographical Sciences, Utrecht University, Utrecht.

700 Hijma, M. P., & Cohen, K. M. (2011). Holocene transgression of the Rhine river mouth area, The
701 Netherlands/Southern North Sea: Palaeogeography and sequence stratigraphy. *Sedimentology*, 58(6), 1453–
702 1485. <https://doi.org/10.1111/j.1365-3091.2010.01222.x>

703 Hijma, M. P., Cohen, K. M., Hoffmann, G., Van der Spek, A. J. F., & Stouthamer, E. (2009). From river valley to
704 estuary: The evolution of the Rhine mouth in the early to middle Holocene (western Netherlands, Rhine-
705 Meuse delta). *Netherlands Journal of Geosciences - Geologie En Mijnbouw*, 88(1), 13–53. Cambridge
706 Core. <https://doi.org/10.1017/S0016774600000986>

707 Hoffmans, G. J. C. M., & Verheij, H. J. (1997). *Scour Manual*. Rotterdam: A.A.Balkema.

708 Hoitink, A. J. F., Wang, Z. B., Vermeulen, B., Huismans, Y., & Kästner, K. (2017). Tidal controls on river delta
709 morphology. *Nature Geoscience*, 10, 637.

710 Huismans, Y., van Velzen, G., O'Mahony, T. S. D., Hoffmans, G. J. C. M., & Wiersma, A. P. (2016). Scour hole
711 development in river beds with mixed sand-clay-peat stratigraphy. *ICSE Conference 2016, Oxford UK*.

712 Huismans, Y., Wiersma, A., Blinde, J., van Kesteren, W., & Mosselman, E. (2013). *Erosie door het verwijderen van*
713 *boomstammen uit de Merwedde* (Definitief No. 1206826-000-ZWS-0020). Deltares.

714 Janssens, M. M., Kasse, C., Bohncke, S. J. P., Greaves, H., K.M. Cohen, undefined, Wallinga, J., & Hoek, W. Z.
715 (2012). Climate-driven fluvial development and valley abandonment at the last glacial-interglacial
716 transition (Oude IJssel-Rhine, Germany). *Netherlands Journal of Geosciences - Geologie En Mijnbouw*,
717 91(1–2), 37–62. Cambridge Core. <https://doi.org/10.1017/S001677460000055X>

718 Kjerfve, B., Shao, C.-C., & Stapor, F. W. (1979). Formation of deep scour holes at the junction of tidal creeks: An
719 hypothesis. *Marine Geology*, 33(1), M9–M14. [https://doi.org/10.1016/0025-3227\(79\)90126-9](https://doi.org/10.1016/0025-3227(79)90126-9)

720 Kuehl, S. A., Allison, M. A., Goodbred, S. L., & Kudrass, H. (2005). The Ganges-Brahmaputra Delta. In: Giosan, L.
721 & J.P. Bhattacharya (Eds.). In *River deltas—Concepts, Models and Examples*. SEPM Special Publication
722 83.

723 Liang, B., Du, S., Pan, X., & Zhang, L. (2020). *Local Scour for Vertical Piles in Steady Currents: Review of*
724 *Mechanisms, Influencing Factors and Empirical Equations*. 8(4). <https://doi.org/10.3390/jmse8010004>

725 Luan, H. L., Ding, P. X., Wang, Z. B., Ge, J. Z., & Yang, S. L. (2016). Decadal morphological evolution of the
726 Yangtze Estuary in response to river input changes and estuarine engineering projects. *Geomorphology*,
727 265, 12–23. <https://doi.org/10.1016/j.geomorph.2016.04.022>

728 Madricardo, F., Foglini, F., Campiani, E., Grande, V., Catenacci, E., Petrizzo, A., ... Trincardi, F. (2019). Assessing
729 the human footprint on the sea-floor of coastal systems: The case of the Venice Lagoon, Italy. *Scientific*
730 *Reports*, 9(1), 6615. <https://doi.org/10.1038/s41598-019-43027-7>

731 Mosley, M. P. (1976). An Experimental Study of Channel Confluences. *The Journal of Geology*, 84(5), 535–562.
732 <https://doi.org/10.1086/628230>

733 Nittrouer, J. A., Mohrig, D., Allison, M. A., & Peyret, A. P. B. (2011). The lowermost Mississippi River: A mixed
734 bedrock-alluvial channel. *Sedimentology*, 58(7), 1914–1934. [https://doi.org/10.1111/j.1365-](https://doi.org/10.1111/j.1365-3091.2011.01245.x)
735 [3091.2011.01245.x](https://doi.org/10.1111/j.1365-3091.2011.01245.x)

736 Odgaard, A. J. (1981). *Transverse Bed Slope in Alluvial Channel Bends*. 107(12), 1677–1694.

737 Ottevanger, W., Blanckaert, K., & Uijttewaal, W. S. J. (2012). Processes governing the flow redistribution in sharp
738 river bends. *Meandering Channels*, 163–164, 45–55. <https://doi.org/10.1016/j.geomorph.2011.04.049>

739 Pandey, M., Ahmad, Z., & Sharma, P. K. (2018). Scour around impermeable spur dikes: A review. *ISH Journal of*
740 *Hydraulic Engineering*, 24(1), 25–44. <https://doi.org/10.1080/09715010.2017.1342571>

741 Pierik, H. J., Busschers, B., & Kleinhans, M. G. (2019). *De rol van resistente lagen in de historische morfologische*
742 *ontwikkeling van het Eems-Dollard estuarium vanaf de 19e eeuw*. Utrecht, the Netherlands: Universiteit
743 Utrecht, Faculteit Geowetenschappen, Departement Fysische Geografie and TNO Geologische Dienst
744 Nederland, Utrecht.

745 Pierik, H. J., Stouthamer, E., Schuring, T., & Cohen, K. M. (2018). *Human-caused avulsion in the Rhine-Meuse*
746 *delta before historic embankment (The Netherlands)*. [https:// doi.org/10.1130/G45188.1](https://doi.org/10.1130/G45188.1)

747 Pierini, J. O., Perillo, G. M. E., Carbone, M. E., & Marini, F. M. (2005). Residual Flow Structure at a Scour-hole in
748 Bahia Blanca Estuary, Argentina. *Journal of Coastal Research*, 21(4 (214)), 784–796.
749 <https://doi.org/10.2112/010-NIS.1>

750 Pons, L. J. (1957). *De geologie, bodenvorming en de waterstaatkundige ontwikkeling van het Land van Maas en*
751 *Waal en een gedeelte van het Rijk van Nijmegen*. Wageningen University, Wageningen.

752 Sloff, C. J., van Spijk, A., Stouthamer, E., & Sieben, A. S. (2013). Understanding and managing the morphology of
753 branches incising into sand-clay deposits in the Dutch Rhine Delta. *Intern. J. of Sed. Res.*, 28, 127–138.

754 Stafleu, J., Maljers, D., Gunnink, J. L., Menkovic, A., & Busschers, F. S. (2011). 3D modelling of the shallow
755 subsurface of Zeeland, the Netherlands. *Netherlands Journal of Geosciences - Geologie En Mijnbouw*,
756 90(4), 293–310. Cambridge Core. <https://doi.org/10.1017/S0016774600000597>

757 Stefani, M., & Vincenzi, S. (2005). The interplay of eustasy, climate and human activity in the late Quaternary
758 depositional evolution and sedimentary architecture of the Po Delta system. *Mediterranean Prodelta*
759 *Systems*, 222–223, 19–48. <https://doi.org/10.1016/j.margeo.2005.06.029>

760 Stouthamer, E., Cohen, K. M., & Gouw, M. J. P. (2011). *Avulsion and its implications for fluvial-deltaic*
761 *architecture: Insights from the Holocene Rhine-Meuse delta*. 97, 215–232.

762 Stouthamer, E., & De Haas, T. (2011). *Erodibiliteit en risico op zettingsvloeiing als maat voor stabiliteit van oevers,*
763 *onderwatertaluds en rivierbodems van de Oude Maas, de Noord en het Spui*. Utrecht: Dept. Fysische
764 Geografie / Universiteit Utrecht.

765 Stouthamer, E., Pierik, H. J., & Cohen, K. M. (2011a). *Erodibiliteit en kans op het ontstaan van zettingsvloeiing als*
766 *maat voor stabiliteit van oevers, onderwatertaluds en rivierbodem van de Lek*. Universiteit Utrecht &
767 Deltares.

768 Stouthamer, E., Pierik, H. J., & Cohen, K. M. (2011b). *Lithologische opbouw van de ondergrond rondom de rivier*
769 *de Lek*. Universiteit Utrecht, Faculty of Geosciences.

770 Stouthamer, Esther, & Berendsen, H. J. A. (2000). Factors Controlling the Holocene Avulsion History of the Rhine-
771 Meuse Delta (The Netherlands). *Journal of Sedimentary Research*, 70(5), 1051–1064.
772 <https://doi.org/10.1306/033000701051>

773 TNO. (2010). DINOloket [Internet Portal for Geo-Information]. Retrieved from DINOloket website:
774 www.dinoloket.nl

775 TNO. (2014). DINOloket [Internet Portal for Geo-Information]. Retrieved from DINOloket website:
776 www.dinoloket.nl

777 Törnqvist, T. E., Weerts, H. J. T., & Berendsen, H. J. A. (1994). Definition of two new members in the upper
778 Kreftenheye and Twente Formations (Quaternary, the Netherlands): A final solution to persistent
779 confusion? *Geologie En Mijnbouw*, 72, 251–264.

780 van der Wegen, M., & Roelvink, J. A. (2012). Reproduction of estuarine bathymetry by means of a process-based
781 model: Western Scheldt case study, the Netherlands. *Geomorphology*, 179, 152–167.
782 <https://doi.org/10.1016/j.geomorph.2012.08.007>

783 Vellinga, N. E., Hoitink, A. J. F., van der Vegt, M., Zhang, W., & Hoekstra, P. (2014). Human impacts on tides
784 overwhelm the effect of sea level rise on extreme water levels in the Rhine–Meuse delta. *Coastal*
785 *Engineering*, 90, 40–50. <https://doi.org/10.1016/j.coastaleng.2014.04.005>

786 Vermeulen, B., Hoitink, A. J. F., & Labeur, R. J. (2015). Flow structure caused by a local cross-sectional area
787 increase and curvature in a sharp river bend. *Journal of Geophysical Research: Earth Surface*, 120(9),
788 1771–1783. <https://doi.org/10.1002/2014JF003334>

789 Vos, P. C., & Cohen, K. M. (2014). Landschapsgenese en paleogeografie. In *BOORrapporten. Twintig meter diep!*
790 *Mesolithicum in de Yangtzehaven-Maasvlakte te Rotterdam*. (pp. 61–146). Moree, J.M., and Sier, M.M.
791 (eds) BOOR Gemeente Rotterdam, Bureau Oudheidkundig Onderzoek Rotterdam, Gemeente Rotterdam.

792 Wang, B., & Xu, Y. J. (2018). Decadal-Scale Riverbed Deformation and Sand Budget of the Last 500 km of the
793 Mississippi River: Insights Into Natural and River Engineering Effects on a Large Alluvial River. *Journal*
794 *of Geophysical Research: Earth Surface*, 123(5), 874–890. <https://doi.org/10.1029/2017JF004542>

795 Wang, C., Yu, X., & Liang, F. (2017). A review of bridge scour: Mechanism, estimation, monitoring and
796 countermeasures. *Natural Hazards*, 87(3), 1881–1906. <https://doi.org/10.1007/s11069-017-2842-2>

797 Weerts, H. J. T., & Busschers, F. S. (2003). *Beschrijving lithostratigrafische eenheid*. Nederlands Instituut voor
798 Toegepaste Geowetenschappen TNO. Utrecht. Retrieved from [https://www.dinoloket.nl/stratigrafische-](https://www.dinoloket.nl/stratigrafische-nomenclator/formatie-van-echteld)
799 [nomenclator/formatie-van-echteld](https://www.dinoloket.nl/stratigrafische-nomenclator/formatie-van-echteld)

- 800 Wiersma, A. P. (2015). *De ondergrond van de Boven Merwede, Dordtsche Kil, Nieuwe Maas en Nieuwe Waterweg*
801 (No. 1208925-000-ZWS-0024). Deltares.
- 802 Zimmermann, C., & Kennedy, J. F. (1978). *Transverse bed slopes in curved alluvial streams*. *104*, 33–48.
- 803